THE JOURNAL OF PHYSICAL CHEMISTRY B

Article

pubs.acs.org/JPCB

Effect of the Architecture on Polyelectrolyte Adsorption and Condensation at Responsive Surfaces

Rita S. Dias* and Alberto A. C. C. Pais

Department of Chemistry, Coimbra University, Rua Larga, 3004-535 Coimbra, Portugal

ABSTRACT: Adsorption profiles and conformational properties of negatively charged polyions at responsive surfaces were investigated by Monte Carlo simulations using a simple coarse-grained model. The surface, carrying both negative and positively charged groups, presents different overall charge, ranging from −10 to +50 *e*, and states, where the surface groups are either in a liquid-like structure (frozen surface) or laterally mobile (fluid surface). Polyions with both linear and ring architectures are considered. We have found that for very attractive surfaces the classical picture of a strongly adsorbed polyion with an extended and flat conformation emerges, independently of the architecture of the polyion or the state of the surface. At weakly attractive surfaces, the ring polyion adsorbs more strongly since it loses less entropy on adsorption than a linear chain. The adsorption of the ring is also enhanced at the fluid surfaces, since its more compact conformation increases the polarization of the surface. However, the linear polyion shows a significant adsorption at a neutral fluid surface, while the ring chains are totally desorbed, suggesting a delicate balance between the entropy of the surface groups and that of the chains. Although ring polyions show a stronger adsorption and a more compact conformation both in- and out-of-plane, at weakly attractive surfaces, no significant influence of the architecture was found on the polyion induced surface polarization (fluid surfaces) or opposite charge patch detection (frozen surfaces), at the monomer level. The adsorption profiles are, however, very different. For linear polyions at weakly attractive surfaces, it was observed a strong predominance of one-tail conformations, which was independent of the state of the surface.

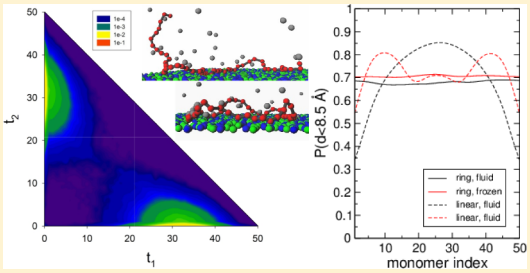

INTRODUCTION

Protein and polymer adsorption onto lipid bilayers and monolayers is fundamentally interesting and has great importance in medicine, biology, and technological applications such as biosensors, implants, food, and pharmaceutical formulations.

These systems have thus been vastly studied using experimental, theoretical, and computer simulation approaches using simple or more complicated model systems. One of the most striking characteristics of surfactants and lipid bilayers is the ability of the individual molecules to react to an adsorbing object as opposed to hard and homogeneous surfaces. The dynamic modes of the individual amphiphilic molecules include lateral diffusion and vertical excursions out of the bilayer and both such modes have been shown to influence the adsorption degree and conformation of interacting macromolecules. Lipid demixing and formation of domains have been observed experimentally, upon the adsorption of DNA,[1−3] peptides,[4] and proteins[5] onto lipid membranes, as well as resorting to computer simulations in protein−membrane[6,7] and polyelectrolyte−membrane[8,9] systems. The demixing of the lipids affects the adsorption isotherm of proteins and protein−protein interaction[10−14] as well as the adsorption ability and degree of compaction of polyelectrolytes[8,9,15] and may lead to counter-intuitive results, such as the adsorption of a negatively charged polyelectrolyte onto a weakly negatively charged surface[8,15] and the stronger adsorption of a flexible polyelectrolyte compared to a more rigid one.[8]

The adsorption of ring chains at surfaces was looked upon, primarily with the intent of assessing the effect of tails in polymer adsorption. It was found, using an extension of the Scheutjens−Fleer theory,[16] that at weak adsorbing surfaces, the ring chains showed larger adsorption than the linear ones. However, the reverse was true at strongly interacting surfaces. At low coverage, the differences in conformational entropy loss on adsorption between rings and linear chains favors the adsorption of ring molecules. At high surface coverage, the formation of tails allows the adsorption of a larger number of polymers. Polymer rings are thus slightly more effectively anchored at the interface but form a thinner layer. Using a different approach, it was found that, due to the closure of the chain, the ring polyions have a more compact structure and are more affected by the surface.[17]

Other, more recent, studies are directed specifically to DNA molecules motivated by the concern that experimental techniques such as atomic force microscopy (AFM), which implies the adsorption of the macromolecules onto a surface, modify the conformational behavior of DNA molecules. As such, the models were chosen to mimic a supercoiled DNA. It has been shown that the conformation of an adsorbed chain depends on the number of helical turns of the chain.[18] A chain with a small number of helical turns shows substantial

Received: April 12, 2012
Revised: June 11, 2012
Published: June 25, 2012

dx.doi.org/10.1021/jp303540q | *J. Phys. Chem. B* 2012, 116, 9246−9254

conformational changes when the attractive surface potential is increased, while a chain that is saturated in terms of the number of helical turns shows no significant differences upon adsorption. In addition, the saturated chain is more strongly adsorbed, presumably due to its most compact state. In another study,[19] where special care was taken to use physical parameters that described DNA more closely, it was shown that the geometric and thermodynamic properties of the supercoiled DNAs on the surface differ significantly from those in solution. In addition, and for calculations performed at higher ionic strength, the simulated structures closely resemble those observed by AFM, while those calculated at a lower ionic strength were similar to solely a minority of the structures observed experimentally.

All the studies described above were conducted using homogeneous attractive surfaces or flattening potentials. However, as discussed above, the characteristics of the surface can largely influence the adsorption and conformation of macromolecules. In this work we resort to Monte Carlo simulations and a simple coarse-grained model of both the polyion and surface to compare the adsorption behavior of polyions of different architectures, ring vs linear, at responsive surfaces.

MODEL AND SYSTEMS

Model. A simple model was adopted to describe the adsorption of polyions from solution onto surfaces containing both positive and negatively charged particles. The polyion is described as a sequence of negatively charged hard spheres (monomers) connected with harmonic bonds with the chain flexibility regulated by angular force terms. When a ring polyion is considered, the end-monomers of the chain are also connected. The polyion counterions are considered in the calculations. The surface is composed of a hard planar wall with embedded positively and negatively charged hard spheres and, in addition, a minimum amount of monovalent simple ions, also treated as charged hard spheres, is introduced to guarantee the electroneutrality of the system. The solvent enters the model only through its relative permittivity.

A rectangular box with box lengths $L_x = L_y = 200$ Å and $L_z = 400$ Å is considered. Hard walls are placed at $z = z_{wall} = -150$ and 150 Å, and the surface groups are restricted to $z = z_{group} = -148.5$ Å, the centers of the surface groups protruding somewhat into the solution. The system is periodic in the x and y directions. We formally investigate the adsorption from a solution with a finite polyion concentration; however, we note that the surface is sufficiently large to make the results representative for the adsorption of a single polyion. A single 50-monomer long polyion is considered, in both ring and linear architectures. The overall charge of the surface is varied by considering different ratios between cations and anions on the surface. Additionally, the fluidity of the membranes is looked upon; surfaces where the groups have random but fixed positions will be referred to as frozen surfaces, and surfaces where the groups are laterally mobile will be referred to as fluid surfaces.

All interactions are taken as pairwise additive. The total potential energy U of the system can be expressed as a sum of four contributions according to

$$U = U_{nonbond} + U_{bond} + U_{ang} + U_{ext} \quad (1)$$

The nonbonded potential energy, $U_{nonbond}$, is given by

$$U_{nonbond} = \sum_{i<j} u_{i,j}(r_{i,j}) \quad (2)$$

where the summation extends over the polyion monomers, simple ions, and surface groups with $u_{i,j}$ representing the electrostatic potential plus a hard-sphere repulsion according to

$$u_{i,j}(r_{i,j}) = \begin{cases} \infty, & r_{i,j} < R_i + R_j \\ \dfrac{Z_i Z_j e^2}{4\pi\varepsilon_0\varepsilon_r}\dfrac{1}{r_{i,j}}, & r_{i,j} \geq R_i + R_j \end{cases} \quad (3)$$

where Z_i is the valence of particle i, R_i the respective radius, $r_{i,j}$ the distance between particles i and j, e the elementary charge, ε_0 the permittivity of vacuum, and ε_r the relative permittivity of the solvent.

Polyion monomers are connected by harmonic bonds, and the bond potential energy of the polyion, U_{bond}, is

$$U_{bond} = \sum_{i=1}^{n-1} \frac{k_{bond}}{2}(r_{i,i+1} - r_0)^2 + \frac{k_{bond}}{2}(r_{n,1} - r_0)^2 \quad (4)$$

where n is the number of monomers, $k_{bond} = 0.4$ N m^{-1} is the force constant of the harmonic bond, and $r_{i,i+1}$ is the distance between two connected monomers, with equilibrium separation, $r_0 = 5$ Å. The second term is present in the ring polyions only.

The angular potential energy, U_{ang}, is given by

$$U_{ang} = \sum_{i=2}^{n-1} \frac{k_{ang}}{2}(\alpha_i - \alpha_0)^2 + \frac{k_{ang}}{2}[(\alpha_j - \alpha_0)^2 + (\alpha_k - \alpha_0)^2] \quad (5)$$

where α_i, α_j, and α_k are the angles formed by the vectors $\mathbf{r}_{i+1} - \mathbf{r}_i$ and $\mathbf{r}_{i-1} - \mathbf{r}_i$, $\mathbf{r}_{n-1} - \mathbf{r}_n$ and $\mathbf{r}_n - \mathbf{r}_1$, and $\mathbf{r}_n - \mathbf{r}_1$ and $\mathbf{r}_1 - \mathbf{r}_2$, respectively. The last term is, again, present solely in the case of the ring polyions. The equilibrium angle $\alpha_0 = 180°$ and the force constant $k_{ang} = 3.4 \times 10^{-24}$ J deg^{-2}.

Finally, the confining external potential energy, U_{ext}, is given by

$$U_{ext} = \begin{cases} \infty, & |z_i| > z_{wall} \\ 0, & |z_i| < z_{wall} \end{cases} \quad (6)$$

For simplicity, the same hard-sphere radius $R_i = 2$ Å is used for the polyion monomers, surface groups, and simple ions. Moreover, all charged species are monovalent. Throughout, $T = 298$ K and $\varepsilon_r = 78.4$.

Systems. In this work we vary (i) the architecture of the polyion (ring vs linear), (ii) the overall charge of the surface, $\Delta Z_s = N_{ct} - N_{an}$, where N_{ct} and N_{an} are the number of cations and anions on the surface, respectively, and (iii) the mobility of the surface groups (fluid vs frozen). The systems will be referred to as "architecture (r or l):ΔZ_s:surface state (fl or fr)"; for example, r:2:fl refers to a ring polyion at a fluid surface with $\Delta Z_s = 2$. $N_{ct} + N_{an}$ is always equal to 1000, giving a hard-sphere area fraction $1000\pi R_s^2/L_xL_y = 0.31$, whereas the net charge ratio is varied from +50 to −10 e.

A brief characterization of the in-plane structure of the surface groups in the unperturbed surface (absence of polyion) has been performed in a previous work.[8]

Simulation Details. All Monte Carlo simulations are performed in the canonical ensemble employing the standard

dx.doi.org/10.1021/jp303540q | J. Phys. Chem. B 2012, 116, 9246−9254

Metropolis algorithm.[20] The long-range electrostatic interactions are handled using the Ewald summation with an extension to slab geometry.[21]

Two different types of MC trial moves are employed for the polyion: single monomer move and translation of the entire chain. For the linear polyions, slithering moves, where one of the end monomers is moved to the opposite end of the chain with biased radial and angular positioning, were also applied. The single particle move is attempted 10 times more often than the other types of moves. The counterions are subjected to translational moves and the surface groups (when fluid) to translational moves restricted to the *xy* plane.

In the case of frozen surfaces, the equilibration of the systems containing the surface groups and the necessary amount of simple ions to ensure electroneutrality are initially performed. The final configuration of the surface groups is used in the subsequent simulations of systems containing now the polyion and respective counterions and the frozen surface groups. Hence, the surface group configurations in these simulations possess a random 2D liquid-like disordered structure.

Each simulation includes an equilibration of at least 2×10^5 trial moves per particle followed by a production run of at least 4×10^6 trial moves per particle. Statistical uncertainties are evaluated by dividing the total simulation into subbatches. All the simulations are performed using the simulation package MOLSIM.[22]

Characterization. Analyses describing (i) the spatial extension and (ii) the conformation of the polyion, (iii) the surface polarization, and (iv) the adsorption profile were used to characterize the interaction of the polyion with the surface. Polyion monomers located within 8.5 Å from the plane of the surface groups were considered to be adsorbed, and the number of adsorbed monomers is denoted by N_{ads}. The extension of the polyion was characterized by its radius of gyration (R_G). In particular, we employed its projection onto the *xy* plane (parallel to the surface) and the *z* axis (perpendicular to the surface) according to

$$\langle R_{G_{xy}}{}^2\rangle^{1/2} = \left\langle \frac{1}{N_{mon}} \sum_{i=1}^{N_{mon}} [(x_i - x_{CM})^2 + (y_i - y_{CM})^2] \right\rangle^{1/2} \quad (7)$$

and

$$\langle R_{G_z}{}^2\rangle^{1/2} = \left\langle \frac{1}{N_{mon}} \sum_{i=1}^{N_{mon}} (z_i - z_{CM})^2 \right\rangle^{1/2} \quad (8)$$

Adsorbed chains were also characterized by the number of their trains, loops, and tails. A train constitutes a sequence of adsorbed monomers, a loop is a sequence of monomers having both ends connected to trains, and a tail is a sequence of monomers having exactly one end connected to a train. Tails are, naturally, only present in the linear polyions.

The polarization of the surface is shown resorting to contour plots of the charge probability distribution on the surface, determined for a fixed and representative polyion conformation, and also evaluated by projecting the center of each adsorbed monomer upon the surface and calculating the average charge found inside an area of radius of 8.5 Å from this projection. The latter was also used for systems with frozen surfaces to evaluate the ability of the polyions to adsorb to positively charged patches.

Adsorption profiles were evaluated by sampling the probability of each monomer to be adsorbed, i.e., to be present at a distance below 8.5 Å from the surface. The number of monomers in each of the tails was also assessed and plotted independently as contour plots, for the linear polyions.

RESULTS AND DISCUSSION

General Adsorption Behavior. The number of adsorbed monomers as a function of the surface net charge at different polyanion architectures and surface group mobilities is shown in Figure 1. As expected, the number of adsorbed polyion

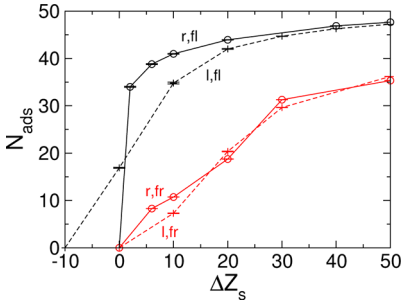

Figure 1. Number of adsorbed monomers, N_{ads}, vs the surface net charge, ΔZ_s, for a system with fluid ("fl", black) or frozen ("fr", red) surface groups and a ring ("r", circles and solid lines) or linear ("l", crosses and dashed lines) polyion. Error bars, representing the standard error of the mean, are given.

monomers decreases as the surface charge becomes less positive. When the surface is overall neutral, only one of the systems presents some adsorption ability, that of the linear polyion at the fluid surface. It is also clear that the desorption from the surface as ΔZ_s decreases is more gradual for the frozen surfaces than for the equivalent fluid systems. Within the fluid surfaces, the ring polyion is the one that shows the more drastic desorption when the surface becomes neutral.

The extensions of the polyion normal and parallel to the surface were also quantified using the root-mean-square (rms) R_G projected onto the *z* axis and the *xy* plane, respectively. Figure 2a shows that $\langle R_{G_z}{}^2\rangle^{1/2}$ increases as the surface becomes more weakly charged, due to the gradual desorption of the polyions from the surface. The set of systems r:ΔZ_s:fl is the least affected by the decrease of ΔZ_s and retains an extension perpendicular to the surface plane $2\langle R_{G_z}{}^2\rangle^{1/2}$ below 10 Å up to $\Delta Z_s = 6$; hence, the polyion is adsorbed in a flat arrangement. Sets of systems l:ΔZ_s:fl and l:ΔZ_s:fr also present a flat polyion conformation but only down to $\Delta Z_s = 20$ and 30, respectively. Figure 2b shows that the polyion extension ($2\langle R_{G_{xy}}{}^2\rangle^{1/2}$) along the surface decreases as the adsorption becomes weaker, varying from around 70 Å for the ring polyion at fluid surfaces to 120 Å for the linear polyion onto a frozen surface, at the higher surface charge net. The set of systems r:ΔZ_s:fl shows again the least variations, nearly none, when the attraction to the surface is decreased, whereas the systems with linear polyions show the largest variation.

In Figure 3, different properties are given as a function of the number of adsorbed monomers with the net surface charge as an implicit parameter, giving thus a more detailed account of the adsorbed state.

Figure 3a displays the number of trains. This property was chosen since it can be directly compared in both polyions; we

dx.doi.org/10.1021/jp303540q | J. Phys. Chem. B 2012, 116, 9246−9254

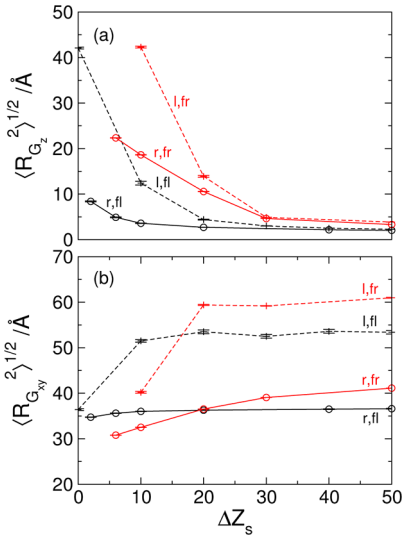

Figure 2. Rms R_G of the polyion projected onto (a) the surface normal and (b) the surface plane vs the surface net charge for a system with fluid ("fl", black) or frozen ("fr", red) surface groups and a ring ("r", circles and solid lines) or linear ("l", crosses and dashed lines) polyion. Error bars, representing the standard error of the mean, are given.

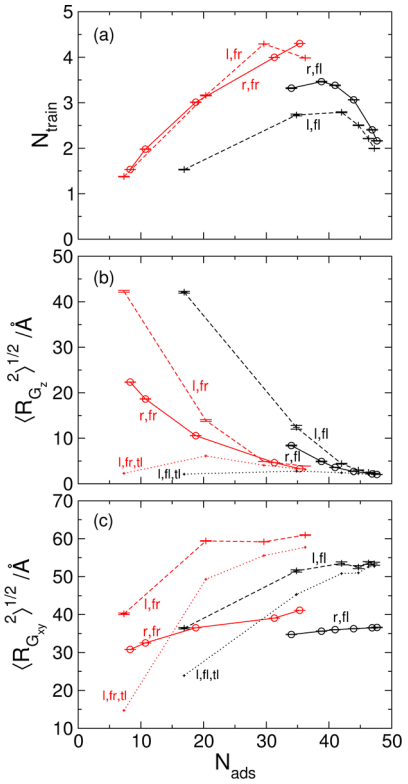

Figure 3. (a) Number of trains and rms R_G of the polyion projected onto (b) the surface normal, and (c) the surface plane vs the number of adsorbed monomers for systems with fluid ("fl", black) or frozen ("fr", red) surface groups and a ring ("r", circles and solid lines) or linear ("l", crosses and dashed lines) polyion. Error bars, representing the standard error of the mean, are given. The dotted lines ("tl") correspond to the rms R_G based on the train and loop monomers of the linear polyion projected onto (b) the surface normal and (c) the surface plane.

recall that ring polyions do not have tails. As the number of adsorbed monomers decreases, there is an initial increase in the number of trains, followed by a decrease. However, some of the systems are only adsorbed for a limited range of monomers and do not show both regimes. The increase of the number of trains as the attraction to the surface diminishes is related to the fact that more loops are present.[23] With further decrease of N_{ads} only a small part of the polyion remains anchored to the surface, which clearly reduces the probability of finding many trains.

Figure 3b shows the rms R_G normal to the surface plane, $\langle R_{G_z}^2\rangle^{1/2}$. It is seen that, as expected, this value increases as the number of adsorbed monomers decreases. For the system with a ring polyion at fluid surfaces this increase is very moderate. Even in the threshold of desorption the polyion keeps a roughly flat conformation. The rms R_G normal to the surface plane calculated, for the linear polyions, taking into account solely the loop and train monomers, $\langle R_{G_z}^2\rangle_{loop,train}^{1/2}$, are depicted in Figure 3b (dotted lines). Clearly, most of the contribution to the $\langle R_{G_z}^2\rangle^{1/2}$ of the linear polyions comes from the tails, since the loops do not extend far from the surface. It is interesting to note that there are, essentially, no differences between $\langle R_{G_z}^2\rangle^{1/2}$ for both ring and linear polyions and $\langle R_{G_z}^2\rangle_{loop,train}^{1/2}$ for larger numbers of adsorbed monomers.

Figure 3c shows the rms R_G parallel to the surface plane, including also the $\langle R_{G_{xy}}^2\rangle_{loop,train}^{1/2}$ of the linear polyions. Similarly to that described in Figure 2b, at decreasing N_{ads}, $\langle R_{G_{xy}}^2\rangle^{1/2}$ also decreases.

As discussed previously,[8] this simple model reproduces the conventional picture that a charged polyion adsorbs in an extended conformation parallel to the surface at strongly attractive surfaces[23,24] and shows a weak adsorption at weakly attractive surfaces, presenting extended tails in the case of linear polyions.[25] The thickness of the layer, given by the length of the polyion tails in this very dilute regime, is determined by the balance between electrostatic attraction to the charged surface and the entropy of the chain.[26] However, the here described model also presents features not appearing in the mean-field theories or in models with homogeneous surface charge densities such as the adsorption of the polyanion onto a neutral surface.

We will now proceed to discuss the results obtained in terms of surface group mobility, polyion architecture, and adsorption profiles.

Effect of Surface Group Mobility. For all considered systems, those with fluid surface groups show a stronger polyion adsorption. When the net surface charge, ΔZ_s, is decreased, the number of adsorbed monomers decreases more slowly for fluid surface groups, implying that the adsorption is more favorable. The enhanced adsorption of the polyion onto fluid surfaces arises, as discussed in previous studies,[8,13] from the ability of the surface charges to adapt to the adsorbed macromolecule. This is clearly shown in Figure 4 which shows the concentration of positive surface groups in the vicinity of an adsorbed ring polyion for system r:2:fl. It is also evident that the polarization of the surface is very local. The polarization effect was quantified by calculating the average charge of the surface in the vicinity of the adsorbed monomers (Figure 5). If the surfaces at study would be homogeneous, the surface charge in an area of radius 8.5 Å would range from 0.00 to 0.57 for ΔZ_s = 0 to 50. Instead it shows variations between ~2.00 and 2.15 for the systems at fluid surfaces. The polarization is thus very significant and more easily achieved at larger surface net charge,

dx.doi.org/10.1021/jp303540q | J. Phys. Chem. B 2012, 116, 9246−9254

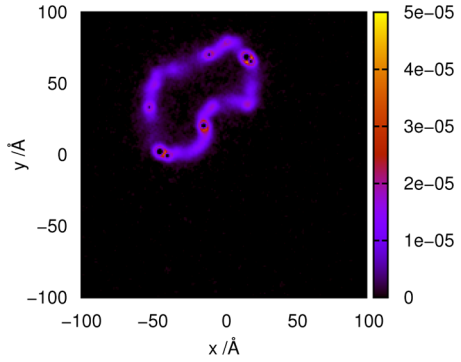

Figure 4. Contour plot of the charge probability distribution on the surface for system r:2:fl, at a fixed polyion position.

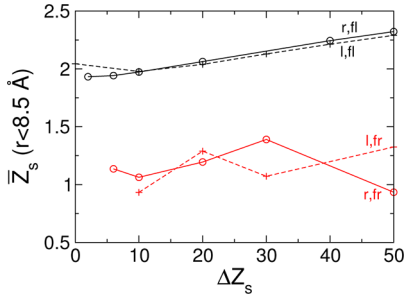

Figure 5. (a) Average charge found in an area of radius 8.5 Å from the in-plane projection of the position of adsorbed monomers of ring ("r", circles and solid lines) and linear ("l", crosses and dashed lines) polyions at fluid ("fl", black) or frozen ("fr", red) surfaces.

although the increase is very moderate. Such types of correlation effects were found to be important in other related systems such as the compaction of DNA by multivalent ions driven by ion-correlation effects[27] and the correlations between surface-adsorbed polyelectrolyte chains in semidilute regimes.[28]

Interestingly, at frozen surfaces, the monomers of the polyion are also adsorbed to positively charged areas of the surface. This is possible, since the surface groups are fixed in a random "liquid-like" conformation.

Regarding the chain conformational indicators, the polyion extension normal to the surface shows, very clearly, that polyions at frozen surfaces present a larger extension for all studied systems (Figure 2a). Regarding the extension parallel to the surface (Figure 2b), it is observed that for $\Delta Z_s > 20$ the polyions onto fluid surfaces are less extended than the corresponding ones in frozen surfaces, which suggests some degree of condensation of the former on the surface and, concomitantly, stronger interaction. For lower values of ΔZ_s the opposite situation is observed, since the systems calculated under fluid conditions present a larger number of adsorbed monomers, which contribute to a greater extension of the polyion at the surface.

A less ambiguous way of interpreting the results is to consider the different indicators at a given number of adsorbed monomers, as represented in Figure 3. It is seen that, for the same number of adsorbed monomers, the polyions at the surfaces with fluid groups present less trains, a larger extension normal to the surface, and a smaller extension parallel to the surface plane than that of the corresponding polyions at frozen surfaces (Figure 3). Taking together these observations, it is suggested that polyions at fluid surfaces present, preferentially, a conformation which is more compact in the *xy* plane and with the *z* contribution to the radius of gyration being mainly due to the tails or longer loops of the linear or ring polyanions, respectively. On the other hand, the polyanion at frozen surfaces shows a more extended conformation parallel to the surface with several anchoring points, possibly to maximize the interaction with the liquid-like frozen surface. Here the $\langle R_{G_z}^2 \rangle^{1/2}$ is expected to decrease, due to the shortening of the tails. Snapshots in Figure 6a,b illustrate this behavior.

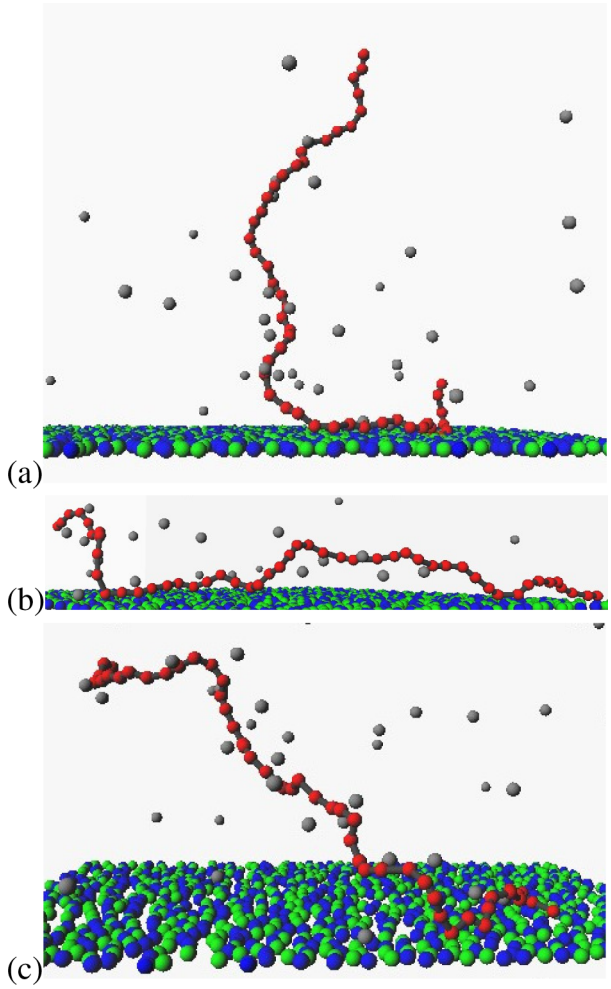

Figure 6. Representative snapshots showing the different behavior adopted by the polyions tails for systems l:0:fl, panel (a), while panels (b) and (c) represent system l:20:fr. Systems l:0:fl and l:20:fr show, on average, N_{ads} = 17 and 20, respectively. The red particles correspond to the polyion monomers, green and blue particles correspond to the positive and negative groups of the surface, respectively, and the gray particles are the simple ions.

Effect of Polyion Architecture. In this section we assess the influence of the polyion architecture on its interaction with surfaces possessing fluid or frozen groups.

At frozen surfaces there are no significant differences between ring and linear polyions, except for the weakly attractive surfaces where the ring polyion adsorbs with a slightly larger number of monomers. This is in good agreement with previous studies[16] and is explained by the fact that a ring loses less entropy on adsorption than a linear chain. Regarding the chain indicators, it is seen, in Figure 3, that the number of trains is very similar for both ring and linear polyions. However, both the polyion extension normal and parallel to the surface are

dx.doi.org/10.1021/jp303540q | J. Phys. Chem. B 2012, 116, 9246−9254

larger for the linear chain than for the ring chain. This together suggests that the differences between the two architectures are due to the fact that the ring polyions are more compact due to the closure of the chain (the rms R_G of the unrestrained polyions in solution are 41.4 ± 0.2 and 60.0 ± 0.8 Å for the ring and linear architectures, respectively), as previously discussed.[17] If we consider adsorption at the "monomer level", by looking at the average charge found in the vicinity of adsorbing monomers (Figure 5), we observe nonmonotonic variations for both architectures around an average value that increases moderately from about 1.0 to ∼1.2. Such fluctuations are probably a consequence that the surfaces do not have the same conformation in all systems. Hence, the polyions at frozen surfaces will likely experience slightly different fields in the different systems. This is corroborated by the fact that no significant differences between sets of systems r:ΔZ_s:fr and l:ΔZ_s:fr are found using the other analyses.

At fluid surfaces a larger difference arises between the adsorption behavior of ring and linear polyions. When the charge of the surface is decreased, the linear polyion desorbs more easily than the corresponding ring chain, up to a very small surface attraction. Two effects may contribute to this behavior: (i) the already discussed fact that ring polyions lose less conformational entropy when adsorbing to a surface, and (ii) the more compact conformation of the ring polyion induces a larger polarization of the surface. A similar phenomenon was previously observed, using similar model systems but where the flexibility of the polyion was varied instead.[8] In this case, and contrarily to what was expected, the more flexible polyion adsorbed more readily to a responsive surface.[8]

It is interesting to note, however, that while the ring polyion is not able to adsorb to the overall neutral fluid surface, about a third of the linear chain is still adsorbed to it. In this case, the entropic penalty of surface patch formation is better compensated by the architecture that shows larger conformational entropy, as shown by the fact that the preferred conformation adopted by the linear polyion is a one-tail conformation (see next section for details).

The different architectures present a different number of trains at fluid surfaces, being slightly larger for the ring polyion at all considered surfaces (Figure 3a). On the other hand, as already seen at the frozen surfaces, the ring polyion shows (i) a slightly smaller vertical extension (Figure 3b) and (ii) a smaller parallel extension (Figure 3c), again due to the more restrained conformation of the ring polyanion, a consequence of the closure of the chain. Representative snapshots in Figure 7 summarize the main observations.

Adsorption Profiles. We have, additionally, looked at the adsorption profiles of the polyions for all considered systems (Figure 8). The top panels refer to the ring polyion at fluid (left) and frozen (right) surfaces. It can be seen that the probability of adsorption of the monomers to the surface is the same along the polyion since the monomers are indistinguishable, contributing equally to the adsorption profile. As expected from the previous discussion, the adsorption probability increases as ΔZ_s increases, and it is also much larger for the polyions at fluid surfaces and the same ΔZ_s. However, if we consider the number of adsorbed monomers (second number in each curve), it is observed, not surprisingly, that the probability of adsorption is equivalent in the two sets of systems.

The profiles obtained for the linear polyions are very different and reflect the importance of the tails in this relatively

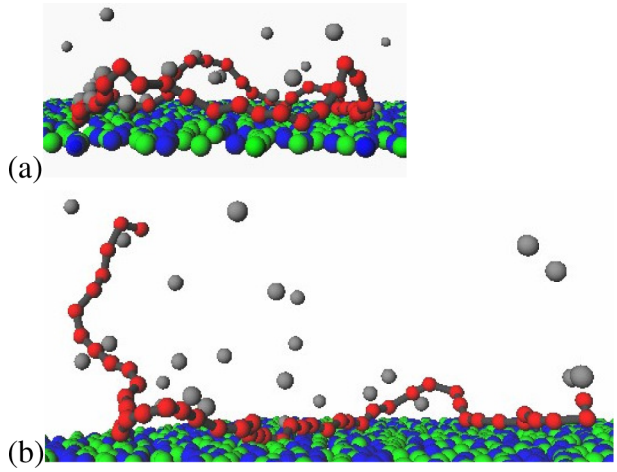

Figure 7. Representative snapshots illustrating the different conformations adopted by the polyions for systems (a) r:2:fl and (b) l:10:fl. The systems show, on average, N_{ads} = 34 and 35, respectively. Color coding as in Figure 6.

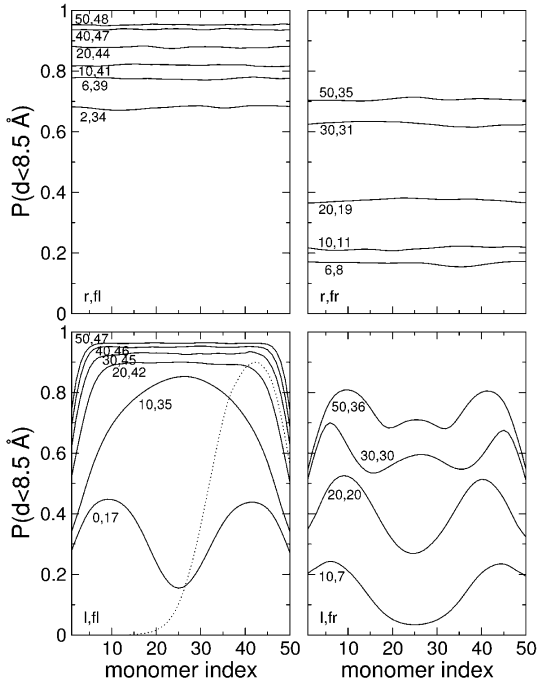

Figure 8. Adsorption profiles, calculated by the probability of finding a specific monomer at a distance below 8.5 Å from the surface groups. The top panels refer to the ring polyions and bottom ones to the linear chains. The panels to the left refer to fluid surfaces and the ones to the right to systems with frozen surfaces. The numbers indicated in each curve are ΔZ_s, N_{ads}.

short polyions. Considering the fluid and more attractive (ΔZ_s > 20) surfaces, it is seen that the probability of adsorption is uniform along most of the chain, but lower at the ends of the polyion, which is attributed to the weaker electrostatic attraction to the surface as well as the increased entropy of the end of the chain. Similar behavior has been observed for polyions adsorbed onto macroions[29] and longer polyions[30,31] of opposite charge. For system l:10:fl the probability of adsorbed monomers decreases further, displaying now a maximum at the center of the chain. System l:0:fl, on the other hand, shows a very different profile, with two maxima close to the ends of the

dx.doi.org/10.1021/jp303540q | J. Phys. Chem. B 2012, 116, 9246−9254

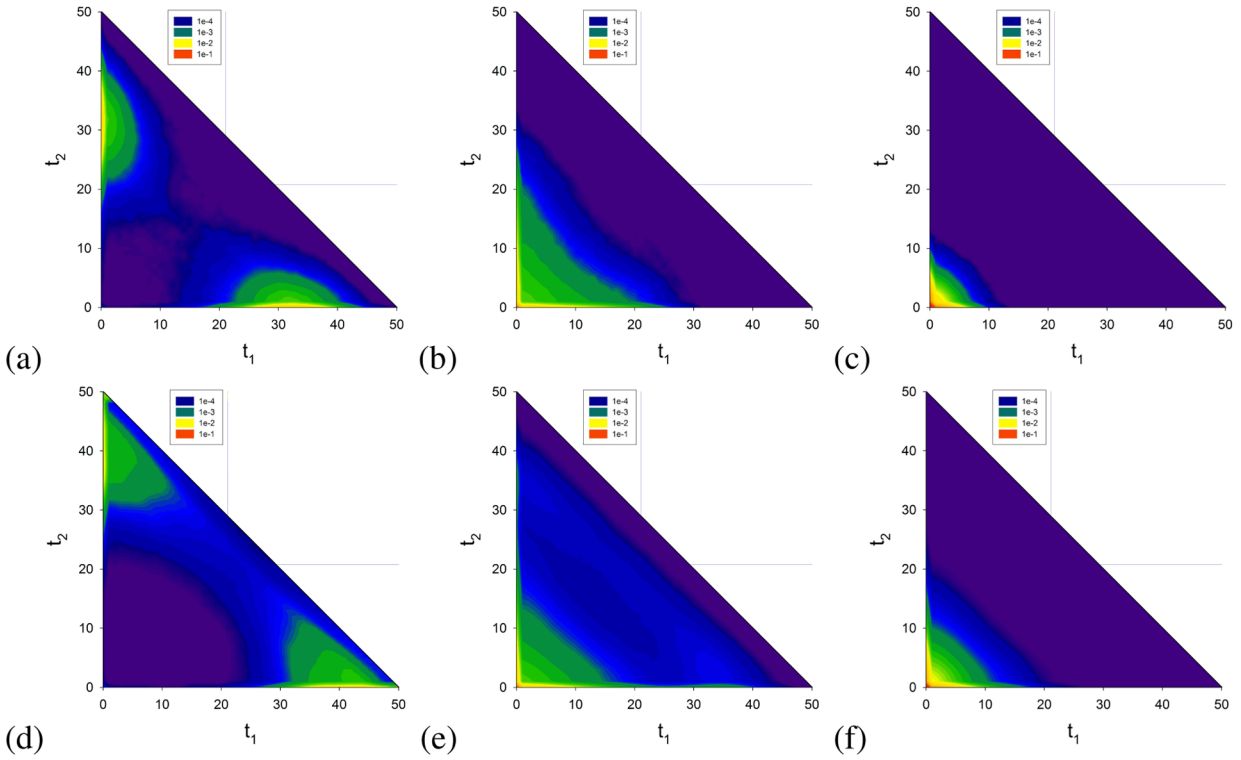

Figure 9. Contour plot of the probability of the number of monomers in each tail, t_1 and t_2, for systems (a) l:0:fl, (b) l:10:fl, (c) l:30:fl, (d) l:10:fr, (e) l:20:fr, and (f) l:30:fr.

chain and a dip in its center. From this profile it would appear that the most likely conformation of the polyion is the adsorption close to the ends and one large loop in the center. However, careful inspection of the snapshots show the predominance of polyion conformations with a very long tail (Figure 6a). The dotted line in Figure 8 shows the adsorption profile of system l:0:fl obtained after a short simulation run, confirming the preference of the polyion to adsorb with one end and display one large tail (asymmetric binding). Since the chain possesses a mirror symmetry, the monomer adsorption also reflects this property, somewhat disguising the effect.

Turning now to the set of systems l:ΔZ_s:fr, we see that for low attractive surfaces the behavior is very similar to what was observed at the fluid surfaces. However, as ΔZ_s is increased, the profile evolves from a double maxima to a three maxima profile, where the middle one shows a lower probability of adsorption than the other two. The profile observed for l:$\Delta Z_s \geq$20:fl is not obtained for frozen surfaces within the studied range of systems. Also note that for systems l:10:fl and l:50:fr, both with about 35 adsorbed monomers, the adsorption profile is different. Such differences corroborate the discussed picture that the polyanion at frozen surfaces adopts a conformation with a larger number of anchoring points (trains), as shown in Figure 3a, presumably to better adapt to the random positively charged patterns of the surface. Since the ends of the chains have a larger conformational entropy than the middle section of the polymers, it is not surprising that the maxima in adsorption located close to the ends of the chain are higher than that in the central part.

To assess the asymmetric binding of the polyion to the surfaces, the probability of the number of monomers in each tail was evaluated and presented individually (t_1,t_2) as contour plots in Figure 9. All the plots are nearly symmetrical, as required by the systems. For system l:0:fl, Figure 9a, the largest probability appears at (0,31) and (31,0) indicating, again, the strong asymmetric binding of the polyion to the surface. Such behavior has been observed previously in systems with a polyion and oppositely charged macroion.[32] It is interesting to note the overwhelming number of conformations with zero monomers in (one of) the tails (note the logarithmic scale). When the fluid surface is made more attractive (ΔZ_s = 10), the largest probability appears now at (t_1,t_2) = (0,0), and it decreases successively at increasing number of monomers in the tails, except for a slightly higher probability of finding polyion conformations possessing one tail of up to 20 monomers. For systems l:30:fl, the probability of finding polyions with none or very short tails is very high. This is in agreement with the adsorption profiles shown in Figure 8 and suggests that there is a one-tail to full-adsorption transition, when the surface becomes more attractive.

The set of systems with frozen surfaces show the same general behavior. System l:10:fr, with maxima in (38,0) and (0,38), presents a strong asymmetric adsorption. A diagonal band connecting the maxima in Figure 9d could indicate a symmetric behavior. However, those probabilities are so low that the system will be classified as an asymmetric one. System l:30:fr is very similar to l:30:fr (Figure 9f and Figure 9c), with the difference that the tails show now a slightly larger number of monomers, in good agreement with the other analyses. System l:20:fr, on the other hand, has common features with both l:30:fr and l:10:fr, showing a large probability for (t_1,t_2) = (0,0) and small maxima for (34,0) and (0,34), i.e., the polyanion adopts, more frequently a conformation that is parallel to the surface, with many trains and loops and small or no tails (Figure 6b). However, it is also possible to find an asymmetric binding of the polyanion to the surface (Figure 6c).

This is an interesting behavior that has not, to our knowledge, been described before. Tails were not considered

dx.doi.org/10.1021/jp303540q | J. Phys. Chem. B 2012, 116, 9246−9254

in the first scaling theories proposed for polymer adsorption at a surface, but their influence in the properties of the systems was quickly recognized.[33−35] Tails, together with the polymer coverage of the surface, can influence the stability of colloidal dispersions by either preventing colloid association (at high coverage) or enhancing it (at low coverages).[34,35] Also, the hydrodynamic thickness of an adsorbing polymer layer is mainly determined by the tails.[33] Behind some of these results were the Scheutjens−Fleer lattice model, where the polymers were described as connected segments which allowed a different description for monomers in the ends or in the center of the chains,[25] and a mean-field theory also developed to account for the effect of the end monomers in a chain.[34,36]

Two major aspects are looked upon in this body of literature: the distribution of monomers away from the adsorbing surface and the conformational aspects of the adsorbing polymer in terms of trains, loops, and tails. The profile of monomer adsorption on a surface is generally found to be a double-layer structure, where the inner layer is built mainly from the loops and the outer one is composed by the tails. Such studies predict, for example, the exchange between an attractive and a repulsive force in two surface systems.[35,36] Regarding the conformational properties of absorbing polymers, the average lengths of tails, loops, and trains have been calculated as a function of a number of parameters, such as polymer length,[37] ionic strength,[38] temperature,[39] and surface curvature.[40] In all these cases, however, the tails of the polymers were not evaluated individually. Hence, the asymmetric binding observed here for weakly attractive surfaces was not pointed out. A tail is the moiety of an adsorbing polymer that shows the largest conformational freedom. Still, the presence of the surface naturally restricts the available space of a polymer tail. The region of configurational space spanned by a single long tail is typically larger than that explored by two tail of a centrally adsorbed polymer.

CONCLUSIONS

A simple coarse-grained model was used to assess differences in the adsorption behavior of ring and linear polyions at responsive surfaces. We have found that both the architecture of the polyion and the characteristics of the surface can influence the adsorption of a polyion.

For very attractive surfaces, the classical picture of a strongly adsorbed polyion with an extended and flat conformation emerges, independently of the state of the surface. Enhanced polyion adsorption was found for all systems when fluid surfaces were considered, including the adsorption of linear polyions at neutral surfaces. Also, fluid surfaces enhance the differences in adsorption between ring and linear polyions.

As expected, at frozen and weakly interacting surfaces, the ring polyion is more strongly adsorbed since it loses less entropy on adsorption than a linear chain. Because of the liquid-like properties of the surface, both polyion are able to adsorb to positively patches on the surface which is reflected in their conformation: a larger number of trains, a longer extension along the surface, and a lower extension normal to the surface. Adsorption at the monomer level is very similar and thus independent of the chain architecture.

At fluid surfaces the more compact conformation of the ring polyion favors the polarization of the surface, enhancing the adsorption of the ring to the surface. Hence, the adsorption of a ring polyion on a fluid surface increases much more drastically when the surface evolves from neutral to weakly charged. However, while the ring polyion does not adsorb to a neutral surface, the linear chain presents about 17 adsorbed monomers, suggesting a delicate balance between the entropy of the surface groups and that of the chains.

Although there are no significant differences in the individual monomer adsorption of ring and linear polyions, the rings generally show a larger adsorption, a more compact conformation in and out-of-plane, and a very different adsorption profile. For linear polyions we have found a strong predominance of one large tail for systems with weakly attractive surfaces, which has not, to our knowledge, been described previously.

AUTHOR INFORMATION

Corresponding Author

*E-mail rsdias@qui.uc.pt; Ph +351 239854464; Fax +351 239827703.

Notes

The authors declare no competing financial interest.

ACKNOWLEDGMENTS

This work was supported by FEDER Funds through the COMPETE program—Programa Operacional Factores de Competitividade (FCOMP-01-0124-FEDER-010831)—and by National Funds through Fundação para a Ciência e Tecnologia (FCT) under the project PTDC/QUI-QUI/101442/2008 and the program Ciência 2007.

REFERENCES

(1) Maier, B.; Radler, J. O. *Macromolecules* **2000**, *33*, 7185−7194.
(2) Kahl, V.; Martin, H.; Maier, B.; Rädler, J. O. *Electrophoresis* **2009**, *30*, 1276−1281.
(3) Leal, C.; Sandström, D.; Nevsten, P.; Topgaard, D. *Biochim. Biophys. Acta* **2008**, *1778*, 214−228.
(4) Denisov, G.; Wanaski, S.; Luan, P.; Glaser, M.; McLaughlin, S. *Biophys. J.* **1998**, *74*, 731−744.
(5) Heimburg, T.; Angerstein, B.; Marsh, D. *Biophys. J.* **1999**, *76*, 2575−2586.
(6) Zhdanov, V. P.; Kasemo, B. *Biophys. Chem.* **2010**, *146*, 60−64.
(7) Dias, R. S.; Linse, P. *Biophys. J.* **2008**, *94*, 3760−3768.
(8) Dias, R. S.; Pais, A. A. C. C.; Linse, P.; Miguel, M. G.; Lindman, B. *J. Phys. Chem. B* **2005**, *109*, 11781−11788.
(9) Tzlil, S.; Ben-Shaul, A. *Biophys. J.* **2005**, *89*, 2972−2987.
(10) May, S.; Harries, D.; Ben-Shaul, A. *Biophys. J.* **2000**, *79*, 1747−1760.
(11) Harries, D.; May, S.; Ben-Shaul, A. *Colloids Surf., A* **2002**, *208*, 41−50.
(12) Hinderliter, A.; May, S. *J. Phys.: Condens. Matter* **2006**, *18*, S1257−S1270.
(13) Mbamala, E. C.; Ben-Shaul, A.; May, S. *Biophys. J.* **2005**, *88*, 1702−1714.
(14) Shi, X.-Q.; Ma, Y.-Q. *J. Chem. Phys.* **2007**, *126*, 125101(1−7).
(15) Fleck, C.; Netz, R. R.; Hennig, H.; von Grünberg, H. *Biophys. J.* **2002**, *82*, 76−92.
(16) van Lent, B.; Scheutjens, J.; Cosgrove, T. *Macromolecules* **1987**, *20*, 366−370.
(17) Stratouras, G. K.; Kosmas, M. K. *Macromolecules* **1991**, *24*, 6754−6758.
(18) Velichko, Y. S.; Yoshikawa, K.; Khokhlov, A. R. *Biomacromolecules* **2000**, *1*, 459−465.
(19) Fujimoto, B. S.; Schurr, J. M. *Biophys. J.* **2002**, *82*, 944−962.
(20) Allen, M. P.; Tildesley, D. J. *Computer Simulations of Liquids*; Clarendon: Oxford, 1987.
(21) Arnold, A.; de Joannis, J.; Holm, C. *J. Chem. Phys.* **2002**, *117*, 2496−2502.
(22) Linse, P. MOLSIM, Version 4.0.0, 2004.

(23) Hoeve, C. A. J.; DiMarzio, E. A.; Peyser, P. *J. Chem. Phys.* **1965**, *42*, 2558−2563.
(24) Silberberg, A. *J. Phys. Chem.* **1962**, *66*, 1872−1883.
(25) Scheutjens, J. M. H. M.; Fleer, G. J. *J. Phys. Chem.* **1979**, *83*, 1619−1635.
(26) Dobrynin, A.; Deshkovski, A.; Rubinstein, M. *Phys. Rev. Lett.* **2000**, *84*, 3101−3104.
(27) Khan, M. O.; Mel'nikov, S. M.; Jönsson, B. *Macromolecules* **1999**, *32*, 8836−8840.
(28) Dobrynin, A.; Rubinstein, M. *Prog. Polym. Sci.* **2005**, *30*, 1049−1118.
(29) Jonsson, M.; Linse, P. *J. Chem. Phys.* **2001**, *115*, 3406−3418.
(30) Dias, R. S.; Pais, A. A. C. C.; Lindman, B.; Miguel, M. G. *J. Chem. Phys.* **2003**, *119*, 8150−8157.
(31) Jorge, A. F.; Sarraguça, J. M. G.; Dias, R. S.; Pais, A. A. C. C. *Phys. Chem. Chem. Phys.* **2009**, *11*, 10890−10898.
(32) Akinchina, A.; Linse, P. *J. Phys. Chem. B* **2003**, *107*, 8011−8021.
(33) Stuart, M. A. C.; Waajen, F. H. W. H.; Cosgrove, T.; Vincent, B.; Crowley, T. L. *Macromolecules* **1984**, *17*, 1825−1830.
(34) Semenov, A. N.; Bonet-Avalos, J.; Johner, A.; Joanny, J. F. *Macromolecules* **1996**, *29*, 2179−2196.
(35) Clément, F.; Johner, A. *C. R. Acad. Sci. Paris* **2000**, *1*, 1135−1142.
(36) Semenov, A. N.; Joanny, J.-F.; Johner, A.; Bonet-Avalos, J. *Macromolecules* **1997**, *30*, 1479−1489.
(37) Scheutjens, J. M. H. M.; Fleer, G. J. *J. Phys. Chem.* **1980**, *84*, 178−190.
(38) Linse, P. *Macromolecules* **1996**, *29*, 326−336.
(39) Sikorski, A. *Macromol. Theory Simul.* **2002**, *11*, 359−364.
(40) Yang, S.; Yan, D.; Shi, A.-C. *Macromolecules* **2006**, *39*, 4168−4174.